UDC 519.6:531.39

B.A. Perviy, O.P. Sarychev

INFLUENCE OF THE MAGNUS EFFECT ON THE SPACECRAFT LIFETIME

A mathematical model of the dynamics of a large fragment of space debris in the form of a ball is developed and investigated. The effect of the Magnus force on the spacecraft lifetime at different angular velocity of object rotation, the apogee of the orbit, the mass of the object, and the radius of the sphere were studied. The dependence of the magnitude of this force on various parameters was studied and a conclusion was made about the insignificant effect of the Magnus effect on the orbital lifetime of the object.
Keywords: space debris, debris removal, Magnus effect

Introduction

Technogenic clogging of near-Earth space is an actual problem of modern space exploration. One of the segments of debris are large fragments of space debris: firstly, these are space vehicles that have stopped their active existence (non-functioning), and, secondly, these are the last stages of carrier rockets. One of the ways to deal with large fragments of space debris is non-contact (without mechanical capture) impact with the aim of moving them to lower orbits for further decay due to aerodynamic braking.

In addition to direct influencing in the opposite direction to the satellite's velocity vector, the incoming atmospheric flux can create an additional perturbing force acting in a plane perpendicular to the oncoming stream [1], [2]. Such an aerodynamic force is described in the literature as the Magnus effect. This phenomenon was a subject of great interest in the field of gas physics and is named after Professor Gustav Magnus, who established that there is a lifting force affecting the rotating cylinder placed in the air stream [3]. The Magnus force is a function of the shape, speed of rotation of the object, density and velocity of freestream flow. As the altitude of the orbit decreases, the density of the atmosphere increases, thereby increasing the magnitude of the force.

 ISSN 1562-9945

As a result, this effect can have a significant effect on the motion of space vehicles in the region of low Earth orbits.

In the study [4], an analysis was made of the possibility of using the Magnus effect to maintain the specified orbit of the object at an ultralow (80 km) height, which, in the opinion of the authors, can improve the quality of atmospheric studies within the ionosphere and thermosphere, and also conduct more controlled escape of objects from orbit.

The results of the study [4] showed that for a spherical object weighing 20 kg, the Magnus effect doubles its time in orbit at a perigee altitude of 80 km and an angular velocity of 5000 rpm.

Problem statement

The purpose of this study is to assess the degree of influence of the Magnus effect on the motion of space objects and to establish the possibility of using it for debris removal due to its own rotation at various characteristics of the object and orbital modes.

Major part

Magnus effect and aerodynamic lift power

The Magnus effect arises at a time when the rotating body creates an asymmetrical flow (above and below the body), thereby creating an aerodynamic rise. As the stream flows around the rotating body, a reduced pressure is created on the side where the flow direction coincides with the direction of the angular velocity of the object (Fig. 1) [5].

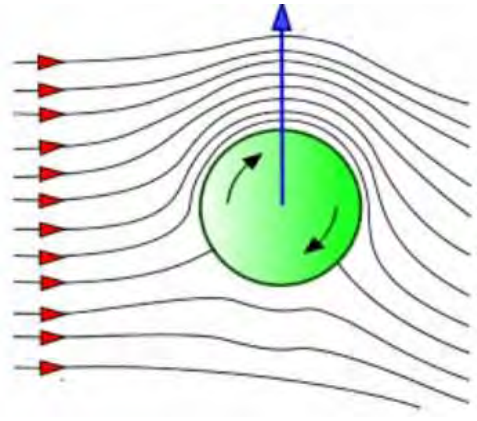

Figure 1 - Magnus force direction in the oncoming stream

The difference in pressure causes a lifting force, which causes the body to move in a direction perpendicular to the oncoming stream. The value and direction of the Magnus force depend on the flux density, and

these dependences are different for the continuum and freestream regimes.

The form of the regime depends on the mean free path of the molecules in the gas. If the mean free path is small in comparison with the dimensions of the body, then the gas can be considered a continuum. With this assumption in mind, the gas density, temperature and velocity of the gas molecules have a definite value at each point of space. In these two regimes, the physics of the flow and the interaction of molecules are different. A widely recognized parameter determining whether the flow is a continuum or a freestream flow is the Knudsen number, which is equal to the ratio of the mean free path to the macroscopic length of the physical object. In other words, the Knudsen number is a measure of the degree of rarefaction of the gas [6]. As the local Knudsen number increases, free-molecular effects become more pronounced and, ultimately, prevail over continual effects. In this study, in contrast to the study [4], the perigee altitude of various orbital regimes exceeds 200 km, so the analysis is under free-molecular conditions of the oncoming flow.

Ashenberg [7] investigated a flat satellite experiencing non-constant aerodynamic perturbations, using the Gauss method for the equations of parameter variation. He states that if the satellite has more flat surfaces, rotates at a certain insignificant speed, or has a large area-to-mass ratio, then the lifting force is not zero. The lifting force is regarded as a vector in a plane perpendicular to the velocity. Perturbations are projected in the direction of the nadir, toward the interior of the orbit, and calculations are performed under the assumption of free-molecular flow. The lift force acting in the plane of the orbit affects the eccentricity, while the orthogonal force perturbs the orbital plane orientation. The general conclusion is that the time-varying aerodynamic resistance can generate different forms of secular orbital motion.

Moore [8] also describes how stabilized satellites can be subjected to a steady or periodic aerodynamic lift, which leads to tangible changes in the parameters of their orbits. He uses Lagrange's equations of motion to study the effect of lift and resistance on orbital elements and states that the exact definition of disturbing forces requires a real experiment, with the study of the interaction of gas with the surface, or a detailed analysis of orbital disturbances and data on the rotation speed.

 ISSN 1562-9945

In [8], a hyperthermal freestream flow, in which the mean free path of molecules is very large in comparison with the dimensions of the satellite and the molecules do not have a random thermal motion (the accommodation coefficient is 1). Diffuse reflection is significant at altitudes of 200-800 km, where atomic oxygen predominates, and at high altitudes the reflection mode is close to mirror reflection.

Wong [9] determines the aerodynamic forces for a rotating sphere in a free-molecular flow. It is established that in the free-molecule regime the Magnus force exerts a negative lift on the spheres in the nadir direction. Expressions for the limiting case of a hypersonic free-molecular flow are derived. Moreover, if the temperature of the sphere is low and the reflection is completely diffusive, the velocity of the reflected molecules is so small compared to the free flow that it can be neglected.

Volkov [10] numerically investigates the behavior of a rotating sphere in a three-dimensional flow of a rarefied gas in a transient and near-continuous flow regime. It is established that in the rarefied gas flow, in the absence of intermolecular collisions, the direction of the Magnus force is opposite to the direction in the continual flow at low Reynolds numbers. The negative rise arising in the transition region is explained by the increase in the contribution of the axial stress to the Magnus force with a decrease in the Knudsen number. The difference in the direction of the Magnus force in the freestream and continual regimes means that in the regime of transient flow the Magnus force depends essentially on the Knudsen number. Moreover, for some value of the Knudsen number this force vanishes. It was shown in [10] that when the Knudsen number decreases, the coefficient in the expression for the Magnus force takes values in the range from -4/3 to the maximum value of +2 in the continuous flow regime at low Reynolds numbers, and then decreases to the limit value corresponding to large numbers Reynolds.

Rubinov and Keller [11] calculate the Magnus force in the continuum regime using the Navier-Stokes equations, and taking into account the small Reynolds numbers. It is shown that for small Reynolds numbers the rotation of the sphere does not affect its coefficient of aerodynamic resistance. In addition, the authors indicate that in the continuum regime for small Reynolds numbers the aerodynamic torque

acting on the rotating sphere does not depend on the translational velocity of the sphere relative to the gas.

Thus, it follows from this review that the coefficient in the expression for the Magnus force in the free-molecular and continual regimes varies from -4/3 to +2 with a decrease in the satellite. Since this study analyzes at altitudes in excess of 200 km, the corresponding coefficient takes negative values.

Equations of motion, perturbing factors and numerical solving methods

We will represent the motion of an artificial Earth satellite as a motion of a material particle of infinitesimal mass in the gravitational field of a central body by a mass under the action of forces determined by a potential function and a set of non-potential forces. Then the differential equations of motion of a particle in an inertial rectangular coordinate system connected with the central body can be represented in the form

$$\frac{d^2\mathbf{x}}{dt^2} = \frac{dU}{d\mathbf{x}} + \mathbf{F}_1,\ U = \frac{fM}{r} + U_1, \tag{1}$$

with initial conditions

$$x_0 = x(t_0),\ \dot{x}_0 = \dot{x}(t_0), \tag{2}$$

where $\mathbf{x} = (x_1, x_2, x_3)^{\mathrm{T}}$ is the position vector of the satellite; $\frac{fM}{r}$ - potential function due to the attraction of a spherical Earth; f - gravitational constant; U_1 - potential function of disturbing forces; r - module of the position vector; t - physical time.

Methods for solving the two-body problem with perturbations include analytical and numerical methods. Numerical approaches imply the numerical integration of perturbing forces. The numerical approach is also applied to the equations of variation of parameters, and in this case the elements of the orbit are integrated numerically [12], [13].

We describe the method and the formulas by which the calculations are performed. We consider the problem of numerical integration of a system of ordinary differential equations of the first order

$$\frac{dx_i}{dt} = f_i\left(x_1, x_2, \ldots, x_n, t\right),\ i = 1, 2, \ldots, n \tag{3}$$

with initial conditions $x_1 = x_1^{(0)}, x_2 = x_2^{(0)}, \ldots, x_n = x_n^{(0)}$ having $t = t_0$

 ISSN 1562-9945

Variables $x_1, x_2, \ldots, x_n$ for convenience we will call the coordinates, and the variable t as time.

The Runge-Kutta formulas given below allow one to determine the coordinates at a point in time $t_{k+1} = t_k + h$ if they are known at the time t_k. The formulas are compiled on the basis of the method of interpolation by polynomials with respect to the step of integration h, in which the terms of some order of smallness are neglected with respect to the step size. In this case, all members are kept up to the 4th order inclusive with respect to the step. The Runge-Kutta formulas have the form

$$
\begin{aligned}
&x_i^{(k)} = x_i(t_k),\\
&p_i^{(k)} = f_i(x_1^{(k)}, x_2^{(k)}, \ldots, x_n^{(k)}, t_k),\\
&q_i^{(k)} = f_i(x_1^{(k)} + \frac{1}{2}hp_1^{(k)}, x_2^{(k)} + \frac{1}{2}hp_2^{(k)}, \ldots, x_n^{(k)} + \frac{1}{2}hp_n^{(k)}, t_k + \frac{1}{2}h),\\
&r_i^{(k)} = f_i(x_1^{(k)} + \frac{1}{2}hq_1^{(k)}, x_2^{(k)} + \frac{1}{2}hq_2^{(k)}, \ldots, x_n^{(k)} + \frac{1}{2}hq_n^{(k)}, t_k + \frac{1}{2}h),\\
&s_i^{(k)} = f_i(x_1^{(k)} + hpr_1^{(k)}, x_2^{(k)} + hr_2^{(k)}, \ldots, x_n^{(k)} + hr_n^{(k)}, t_k + h);
\end{aligned}
\tag{4}
$$

$$
x_i^{k+1} = x_i^{(k)} + \frac{1}{6}h(p_i^{(k)} + 2q_i^{(k)} + 2r_i^{(k)} + s_i^{(k)}), \quad i = 1, 2, .., n \tag{5}
$$

Because of the presence of various perturbing forces, equation (3) can only be used as an approximation of real motion. The accuracy of the approximation decreases as the integration time increases. These perturbing forces include terrestrial gravitational harmonics (deviations from the ideal sphere), lunar-solar gravitational perturbations, atmospheric resistance, solar radiation pressure and the tides of the Earth.

As a model of the Earth's attraction, the standard form of recording the potential of the Earth's gravity was used [14].

Atmospheric drag is the main non-potential force acting on a satellite in low Earth orbit. It acts in the direction opposite to the velocity vector, and reduces the energy of the satellite. A decrease in energy leads to a decrease in the orbit altitude, until the satellite enters the atmosphere. Perturbations caused by atmospheric resistance are considered more significant than the perturbations from - the second zonal harmonic of the Earth from the contribution to the decrease in the altitude of the orbit [14].

Acceleration due to atmospheric drag can be expressed as

$$
\vec{\partial}_{drag} = -\frac{1}{2}\rho\frac{C_d A}{m}v^2\vec{\mathbf{v}}, \tag{6}
$$

where ρ is the density of the atmosphere; C_d - drag coefficient; A - cross-sectional area; m - mass of the satellite; υ - speed of the satellite relative to the atmosphere; $\vec{\mathbf{v}}$ - is the unit vector in the direction of the flow velocity.

Another one of the non-gravitational perturbations is the light pressure. We will assume that the power of the solar radiation flux is constant, the light pressure force is always directed along the Earth-Sun line, the Earth's orbit is circular, the satellite has a spherical shape. Under these assumptions, the acceleration of the direct light pressure of the sun onto the satellite can be given by the formula [15]

$$\vec{\mathbf{a}} = -C_r \frac{A K \varphi}{m c} \left(\frac{1}{R_{AU}} \right)^2 \vec{\mathbf{r}}_s, \tag{7}$$

where $\vec{\mathbf{a}}$ – is the acceleration vector in inertial coordinates; C_r - coefficient of reflectivity; A - the area of the satellite; K - percentage of the emitted light of the Sun, relative to the satellite, which is not eclipsed (usually equal to 1); m - mass of the satellite; φ - solar flux per 1 astronomical unit; c - speed of light; R_{AU} - the distance from the satellite to the Sun in astronomical units; $\vec{\mathbf{r}}_s$ is the unit vector of the position of the Sun, relative to the satellite.

The Magnus force is represented by the expression

$$F_m = \frac{1}{2} C_l \pi r^3 \rho \omega \upsilon, \tag{8}$$

where r is the radius of the spherical object; ρ - density of the oncoming stream; ω - angular velocity of the object; υ is the speed of the oncoming stream.

The Magnus force coefficient C_l, according to [5], [9], [10], is negative for the free-molecular incoming flow and depends on the accommodation coefficient α_τ in the form

$$C_l = -\frac{4}{3} \alpha_\tau. \tag{9}$$

As a potential approach, we assume the limiting case of a hypersonic free-molecular flow with total reflection, under which $\alpha_\tau = 1$ [9].

Modeling the motion of a rotating sphere

The rotating sphere dynamics model is implemented using the Analytical Graphics Systems Tool Kit (AGI STK) software [16]. During

 ISSN 1562-9945

developing the model of a rotating object, the Magnus force is programmed as a super efficient engine with a $2 \cdot 10^{12}$ pulse and 5 kg weight, while the amount of fuel consumed does not affect the final result of the calculations.

Numerical integration of the equation of motion of the satellite with the use of the Magnus effect is represented by Runge-Kutta-Felberg method of 4th order with accuracy control of the 5th order [12], the resistance coefficient, atmospheric density is calculated on the basis of the model of the atmosphere NRLMSISE-00 [17] model of the Earth JGM3 [18], [19].

Results of simulation modeling

The graphs and numerical values of the results of the study are shown in Fig. 2-8 and in Table. 1 to 7, respectively.

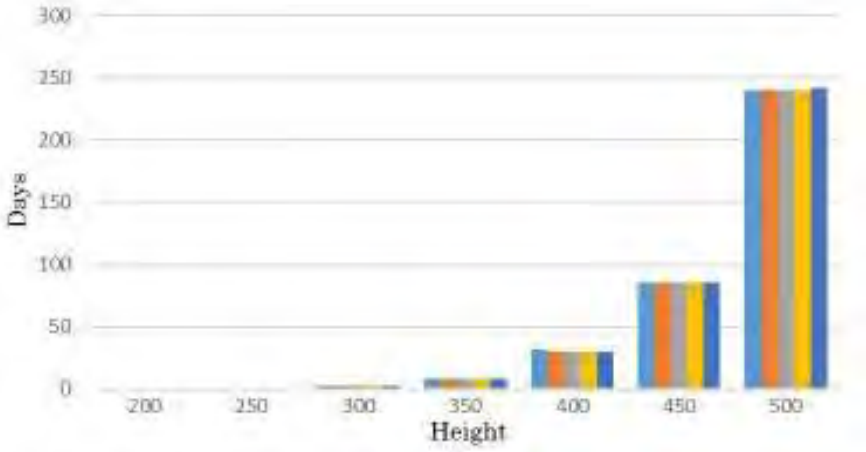

Figure 2 - Comparative histogram of the object lifetime (numerical values in Table 1)

Table 1

The object lifetime (days) on orbit at different angular velocities

Object ang. velocity, rev/min	Lifetime in days for different altitudes, km						
	200	250	300	350	400	450	500
w/o rotation	0,09	0,51	2,39	8,41	31,4	85,6	239,6
1000	0,09	0,51	2,27	8,42	29,6	85,6	239,6

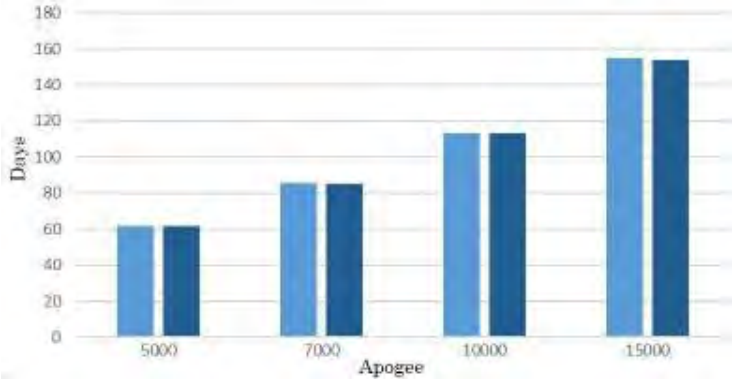

Figure 3 - Comparative histogram of the object lifetime on orbit at perigee 200 km

Table 2

The object lifetime (days) on orbit at perigee 200 km

Object ang. velocity, rev/min	Lifetime in days for different apogee altitudes, km			
	5000	7000	10000	15000
w/o rotation	61,8	85,4	113,2	154,5
1000	61,6	85,2	112,9	153,9

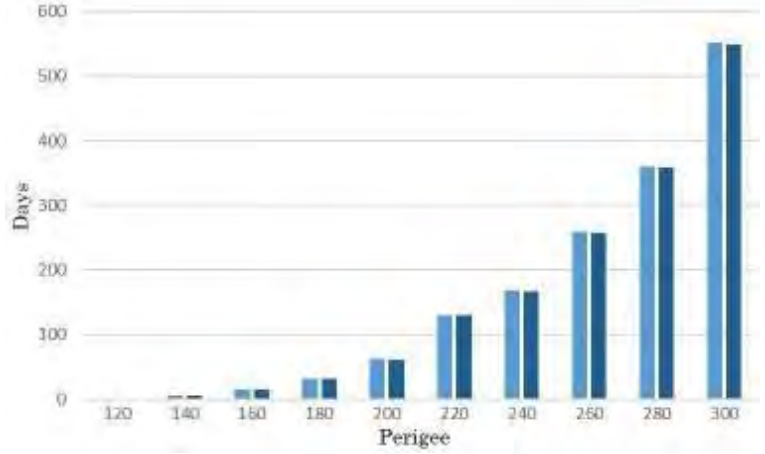

Figure 4 - Comparative histogram of the object lifetime on orbit at 5000 km apogee

Table 3

The object lifetime (days) on orbit at 5000 km apogee

Object ang. velocity, rev/min	Lifetime in days for different perigee altitudes, km					
	200	220	240	260	280	300
w/o rotation	61,8	130	168	258	360	552
1000	61,6	130	167	257	359	548

 ISSN 1562-9945

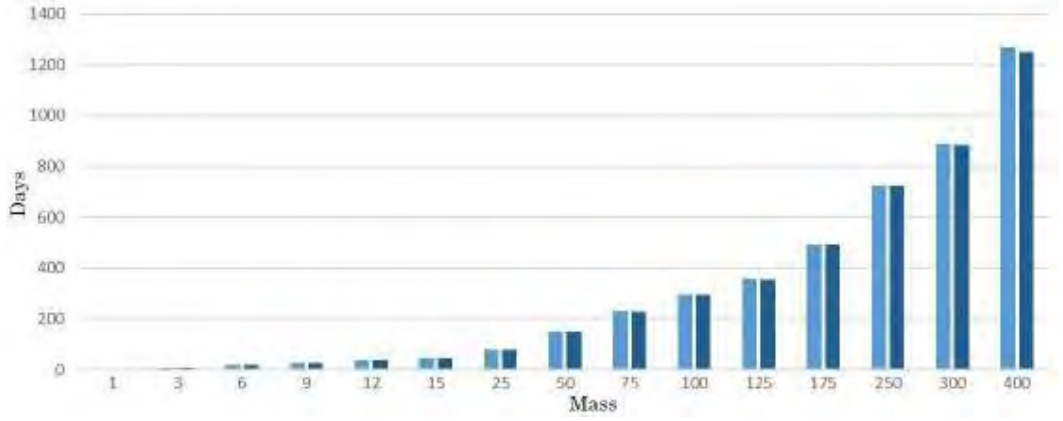

Figure 5 - Comparative histogram of the object lifetime due to different object masses on orbit at 5000 km apogee

Table 4

The object lifetime (days) at different mass on orbit at apogee 5000 km

Object ang. velocity, rev/min	Lifetime in days for different object mass, kg														
	1	3	6	9	12	15	25	50	75	100	125	175	250	300	400
w/o rotation	2,9	8,5	17,9	27,4	36,2	45,4	77,5	150	230	294	357	493	725	887	1269
1000	2,9	8,5	17,9	27,4	36,1	45,4	77,3	150	229	294	356	492	723	884	1250

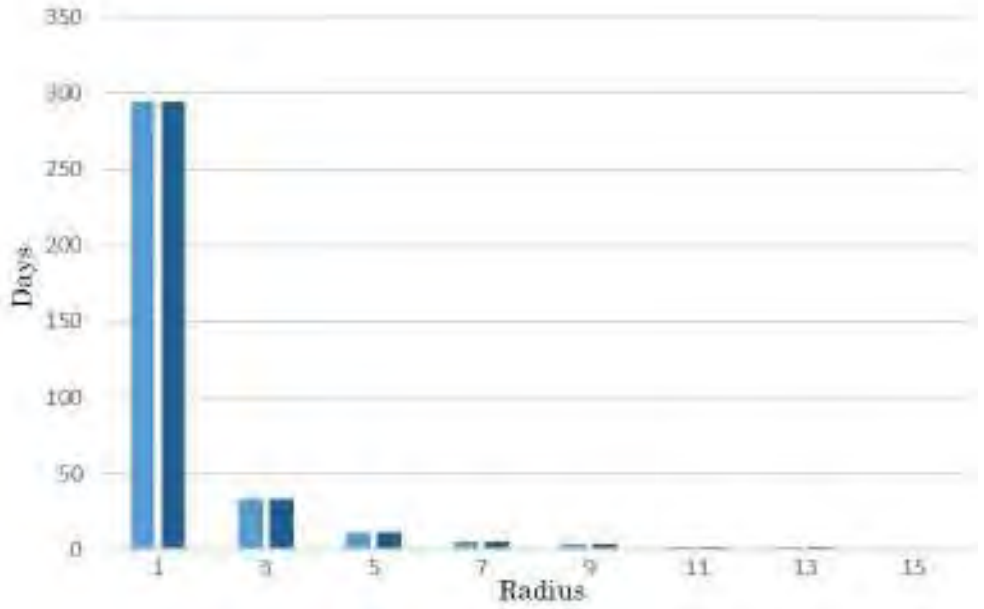

Figure 6 - Comparative histogram of the object lifetime due to different object radius at apogee 5000 km, perigee 200 km, weight 100 kg

Table 7

The object lifetime (days) at different object radius at apogee 5000 km, perigee 200 km, mass 100 kg

Object ang. velocity, rev/min	Lifetime in days depending on different object radius, m			
	1	3	5	7
w/o rotation	294,3	33,5	11,5	5,7
1000	294,1	33,3	11,4	5,6

Conclusions

A mathematical model of the dynamics of a large fragment of space debris in the form of a ball is developed and investigated, taking into account its motion relative to the center of mass. On the basis of the constructed model, the influence of the Magnus force on the time of finding a spherical object in orbit was studied. The dependence of the magnitude of this force on various parameters-the orbital regime, the angular velocity of the object's rotation, the mass, and the radius of the sphere are investigated. Taking into account the accepted height of the final removal of the object in 200 km, it is possible to state with confidence that within the framework of the model built, the Magnus effect does not significantly affect the orbital time of the object in orbit, regardless of the size of the object and the orbital mode.

REFERENCES

1. Pulido C. L. Aerodynamic Lift and Drag Effects on the Orbital Lifetime Low Earth Orbit (LEO) Satellites / C. L. Pulido. – University of Colorado Boulder, 2007.

2. Cook G. E. The Effect of Aerodynamic Lift on Satellite Orbit / G. E. Cook // Plant. Space Science. – 1964. – Vol. 12. – P. 11.

3. Borg K. I. Force on a Spinning Sphere Moving in a Rarefied Gas / K. I. Borg, L. H. Soderholm, H. Essen // Physics of Fluids. – 2003. – Vol. 15, № 3. – P. 736–741.

4. Ramjatan S. Magnus Effect on a Spinning Satellite in Low Earth Orbit / S. Ramjatan, N. Fitz-Coy, A. Yew // AIAA/AAS Astrodynamics Specialist Conference. – 2016.

5. Borg J. Magnus Effect: An Overview of its Past and Future Practical Applications / J. Borg. – Washington D. C.: NAVSEA. – 1986.

 ISSN 1562-9945

6. Roy S. Modelng Gas Flow Through Microchannels and Nanopores / S. Roy, R. Raju, H. F. Chuang, B. A. Cruden, M. Meyyappan // Journal of Applied Physics. – 2003. – Vol. 93, № 8. – P. 10.

7. Ashenberg J. On the Effects of Time-Varying Aerodynamics Coefficients on Satellite Orbits / J. Ashenberg // Acta Astronautica. – 1996. – Vol. 38, № 2. – P. 75–86.

8. Moore P. The Effect of Aerodynamic Lift on Near-Circular Satellite Orbits / P. Moore // Planet, Space Sciences. – 1985. – Vol. 33, № 5. – P. 479–491.

9. Wang C. T. Free Molecular Flow Over a Rotating Sphere / C.-T. Wang // AIAA. – 1972.

10.Volkov A. Aerodynamic coefficients of a Spinning Sphere in a Rarefied-Gas Flow / A. Volkov // Izvestiya Rossiiskoi Akademii Nauk. – 2009. – Vol. 44, № 1. – P. 167–187.

11.Rubinow S. I. The Transverse Force on a Spinning Sphere Moving in a Viscous Fluid / S. I. Rubinow, J. B. Keller // Journal of Fluid Mechanics. – 1961. – Vol. 11, № 3. – P. 12.

12.Hall T. S. Orbit maneuver for responsive coverage using electric propulsion / T. S Hall // Air Force Institute of Technology, 2010.

13.Liu J. J. F. The Orbit Decay and Lifetime (LIFTIM) Prediction Program / J. J. F. Liu, R. L. Alford // Northrop Services, Inc., 1974.

14.Chobotov V. Orbital Mechanics / V. Chobotov // Virginia: AIAA. – 2002.

15.Довідкова система AGI STK / Solar Radiation Computation. – Режим доступу до сист. http://help.agi.com/stk/index.htm#gator/eq-solar.htm

16.Пакет инженерного моделювання AGI STK. – Режим доступу до сист. http://www.agi.com/products /engineering-tools

17.Picone J. M. NRLMSISE-00 empirical model of the atmosphere: Statistical comparisons and scientific issues / J. M. Picone, A. E. Hedin, D. P. Drob, A. C. Aikin // Journal of geophysical research. – 2002. – Vol. 107, № A12. – P. 1468.

18.McCarthy D. D. IERS Conventions (IERS Technical Note; 21) / Dennis D. McCarthy // Central Bureau of IERS: Paris. – 1996. – Режим доступу до ресурсу https://www.iers.org/SharedDocs/Publikationen/EN/ IERS /Publications /tn/ TechnNote21/tn21_40.pdf?__blob=publicationFile&v=1

19.Saunders A. A New Tool for Satellite Re-entry Predictions / A. Saunders // 5th European Conference of Space Debris, 2009. – Darmstadt, 2009.